S. Luca

J. L. Santailler[1]
e-mail: jean-louis.santailler@cea.fr

J. Rothman

J. P. Belle

C. Calvat

G. Basset

A. Passero

Commissariat à l'Energie Atomique,
LETI – MINATEC,
17 Rue des Martyrs,
38054 Grenoble Cedex 9, France

V. P. Khvostikov

N. S. Potapovich

R. V. Levin

Ioffe Physico-Technical Institute,
26 Polytechnicheskaya,
194021 St. Petersburg, Russia

GaSb Crystals and Wafers for Photovoltaic Devices

GaSb *material presents interesting properties for single junction thermophotovoltaic (TPV) devices.* GaSb:Te *single crystal grown with Czochralski (Cz) or modified Czochralski (Mo-Cz) methods are presented and the problem of Te homogeneity discussed. As the carrier mobility is one of the key points for the bulk crystal, Hall measurements are carried out. We present here some complementary developments based on the material processing point of view: the bulk crystal growth, the wafer preparation, and the wafer etching. Subsequent steps after these are related to the p/n or n/p junction elaboration. Some results obtained for different thin-layer elaboration approaches are presented. So from the simple vapor phase diffusion process or the liquid phase epitaxy process up to the metal organic chemical vapor deposition process we report some material specificity.* [DOI: 10.1115/1.2734570]

Keywords: GaSb, bulk crystal growth, LPE, MOCVD, thermophotovoltaic

1 Introduction

For production of highly effective photoconverters, good semiconductor materials quality with strictly determined parameters are required. For GaSb thermophotovoltaic (TPV) cells an homogeneous Te-doping level in the bulk semiconductor of $(2-8)10^{17}$ cm^{-3} is required to produce high efficient PV cells by the Zn diffusion process [1–5]. In this paper we propose to compare crystals grown by different methods and wafers prepared by different teams, to investigate some bulk material properties, and to present different approaches for thin-layer elaboration by metal organic chemical vapor deposition (MOCVD) or liquid phase epitaxy (LPE). We also present the p/n junction obtained on Te doped GaSb wafer (n type) with a thin Zn buffer layer (p type) obtained by vapor phase diffusion, and n/p junction based on low Te doped GaSb wafer (p type) with a thin Te layer (n type) obtained by LPE. It is apparent that improvement of ingots properties, wafers, and "buffer" layers is of great importance for fabrication of future cells.

2 Growth of GaSb Ingots

2.1 GaSb:Te Bulk Growth

2.1.1 Czochralski Technique. Among different crystal growth methods, the classical Czochralski process is widely used for gallium antimonide semiconductor compounds [6–16]. A French team developed such a technique for the growth of single GaSb:Te crystals, 2 in. in diameter and more than 100 mm in length. Crystals were grown from home made seeds oriented in the ⟨100⟩ direction [15]. For TPV application the tellurium concentration in the bulk material must be in the range of $(2-8)\cdot 10^{17}$ cm^{-3}. The segregation coefficient (k), represents the ratio between Te concentration in the solid phase (Cs) over the Te concentration in the liquid phase (Cl) at the solid/liquid interface during the growth. Assuming that k=Cs/Cl of Te in GaSb is ~0.37 [17,18], the Te concentration in the crystal will continuously vary during the growth and only part of the crystal will mach the specifications. So the main problems were to fix the initial Te concentration in the raw material and to optimize growth conditions which allow Te homogeneity in both radial and axial directions in most of the crystal.

For this it is necessary to prepare a polycrystalline GaSb charge from high-purity raw materials, Ga, Sb, and Te in a closed silica ampoule sealed under secondary vacuum. The initial Te concentration is intentionally increased by a factor of 10–15 in the charge. The ampoule is then heated by 150–200 °C over a GaSb melting point (712 °C) for 12 h with different mechanical stirring movements in order to homogenize the melted material. Then the ampoule is cooled down in a directional thermal gradient to solidify the ingot and to avoid silica breakings. The whole 9 kg per run of polycrystalline charge is prepared and etched before being installed inside a 6 in. silica crucible. The crucible is placed inside a graphite holder which is part of the thermal core zone used for GaSb single-crystal growth. The furnace is heated by a radio-frequency generator operating in the 10 kHz range. The furnace is pumped several hours under secondary vacuum at low-power level in order to favor the pumping process. Afterward, an argon pressure of 1 atm is fixed in the chamber. The GaSb charge is heated up and stabilizes near the melting point. Some particles, mainly oxide compounds, may be present at the surface of the melt. The GaSb vapor pressure is not negligible at this tempera-

[1]Corresponding author.

Contributed by the Solar Energy Division of ASME for publication in the JOURNAL OF SOLAR ENERGY ENGINEERING. Manuscript received December 9, 2005; final manuscript received July 19, 2006. Review conducted by Antonio Marti Vega.

Fig. 1 As grown GaSb:Te crystal Se_127 grown by Cz process

ture, leading to a continuous evaporation of the melt. The following parameters are used in the growing process: crystal pulling rate (4–15 mm/h), crystal rotation (5–10 rpm), and crucible rotation (1–5 rpm) are adjusted manually. As the GaSb liquid density (6040 kg/m^3) is greater than GaSb solid density (5610 kg/m^3) the typical crystal weight regulation used for oxide crystal does not work properly. Typical crystals of 2–4 kg, 150–200 mm in length, 40–80 mm in diameter were achieved (see Fig. 1).

Constant crystal diameter is not yet achieved with the explored parameters, due to the high probability of twin formation with ⟨100⟩ seed orientation in the crystal shoulder. A precise growth angle control will help to overcome this problem. After growth, crystals are first etched and then cut with a multidicing saw. The cutting direction is the {100} plane, perpendicular to the growth axis.

Raw wafers with a thickness of 1–1.2 mm are necessary because GaSb single crystals are brittle and ⟨100⟩ substrates are easily cleaved during handling. Further polishing and etching steps are described in the following subsections.

2.1.2 Other Growth Processes. Other *n*-GaSb:Te wafers have been fabricated by the Russian team from ingots grown by a modified Czochralski technique (for more details see Ref. [19]) with optimized temperature and dynamic growth conditions. The growth was carried out in the (100) direction under hydrogen flow. Such conditions permit us to avoid liquid encapsulation, which reduce contamination of melts and ingots.

In fact the two Czochralski processes are rather similar in terms of thermal configuration and thermal gradient at a solid/liquid interface. They differ on the growth parameters used and on the growth atmosphere. We also used a vertical bridgman–liquid encapsulated (VB–LE) process for one sample. With this method we measured a low thermal gradient (10 K/cm) at the solid / liquid interface.

2.2 GaSb:Te Bulk Material Properties. We propose to compare by subsequent analyses wafers grown by VB–LE, and wafers obtained by Cz and Mo-Cz techniques. One is intentionally undoped and the others are Te compensated. Hall measurements were conducted both at IOFFE and at CEA on different wafers.

2.2.1 Hall Type Measurements of p Type Samples. The undoped GaSb sample VB2-4 oriented ⟨100⟩ is cut from an ingot obtained by the encapsulation method (VB–LE) [14,15]. We used LiCl–KCl salt as an encapsulant. Hall measurements were conducted on one sample from 30 K to 300 K. Some results presented in Fig. 2 reveal that the material is *p* type with a net acceptor carrier concentration Na–Nd of 1.36×10^{17} atm/cm^3 at 300 K and a hole mobility μ_h of 650 $cm^2/(V\,s)$ at 300 K. This intrinsic *p* type behavior is due to a high level of residual acceptors identified as $V_{Ga}Ga_{Sb}$ complexes [16].

The second GaSb:Te sample Se_108-2 is intentionality Te doped. The sample is grown by the Czochralski method under argon atmosphere. As the Te target is $3-8\times10^{17}$ atm/cm^3 the Hall results show that the material is also *p* type with a net acceptor carrier concentration Na–Nd of 4.0×10^{16} atm/cm^3 at 300 K, and a hole mobility μ_h of 553 $cm^2/(V\,s)$ at 300 K.

Results obtained on the sample Se_108-5 at IOFFE and at CEA on Se_108-2 are quite similar. Another complementary chemical analysis like induced coupled plasma (ICP) confirmed the tellurium content in the crystal. These results are also in good agreement with Pino's paper [20] who showed that the limit between GaSb:Te *p* and *n* type is in the range of 10^{17} atm/cm^3 of Te. Due to Te concentration, it is logical that Se_108 samples are *p* type.

2.2.2 Hall Type Measurements of n Type Samples. As the initial Te concentration in the melt was not enough we increased it by a factor of ten. After growth with the same melt, the GaSb:Te polycrystalline sample Se_125-A and the single crystal Se_127-A presented quite the same results.

The Hall measurement results showed that the material is *n* type with a net donor carrier concentration Nd–Na of 5.3×10^{17} atm/cm^3, and an electron mobility μ_e of 2767 $cm^2/(V\,s)$ at 300 K. In Fig. 2(*a*) we can see the net carrier concentration of the three samples as function of the temperature, and in Fig. 2(*b*) the mobility variation versus temperature.

A deeper Hall measurements investigation obtained at IOFFE on GaSb:Te samples grown by the Mo-Cz method showed that they are characterized by gradual variation of doping impurity concentration and electron mobility along an ingot (Fig. 3). It is seen from the Hall measurements at 77 K that the electron mobility increases along the ingot 1.5–2 times with the increase of electrically active impurity concentration.

The concentration gradient from $2\cdot10^{17}\,cm^{-3}$ to $(4-6)\cdot10^{17}\,cm^{-3}$ (300 K) of the electrically active impurities along the ingot is, apparently, associated with the rise of the Te concentration of the melt during the growth. The carrier mobility value may serve as an indicator of impurities. It increases toward the end of the ingot. Its rise, in spite of the tellurium concentration increase, may be explained by the reduction of the uncontrolled impurities and clusters content during the crystal growth.

The transverse inhomogeneity of the wafer (Fig. 4) for Te concentration and carrier mobility is 20–30% (for two perpendicular directions). That insignificant inhomogeneity does not influence the main characteristics of TPV cells. Taking into account that acceptable carrier concentration is in the range of $(2-8)\cdot10^{17}\,cm^{-3}$, the GaSb tested ingots can be used for fabrication of high-efficiency TPV cells.

2.2.3 Investigated Samples. Table 1 presents the list of investigated samples and the main Hall results obtained.

In order to simply check the Te incorporation inside the crystal, we also measured the thicknesses after etching and the electrical resistivity of 23 wafers cut from the Se_127 ingot. The wafer electrical resistivity was measured with a classical four point

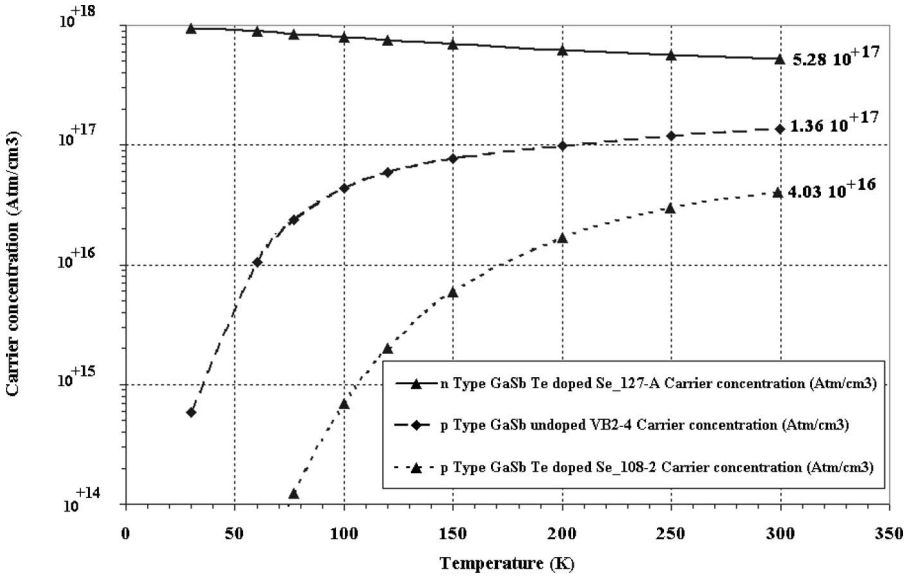

(*a*)

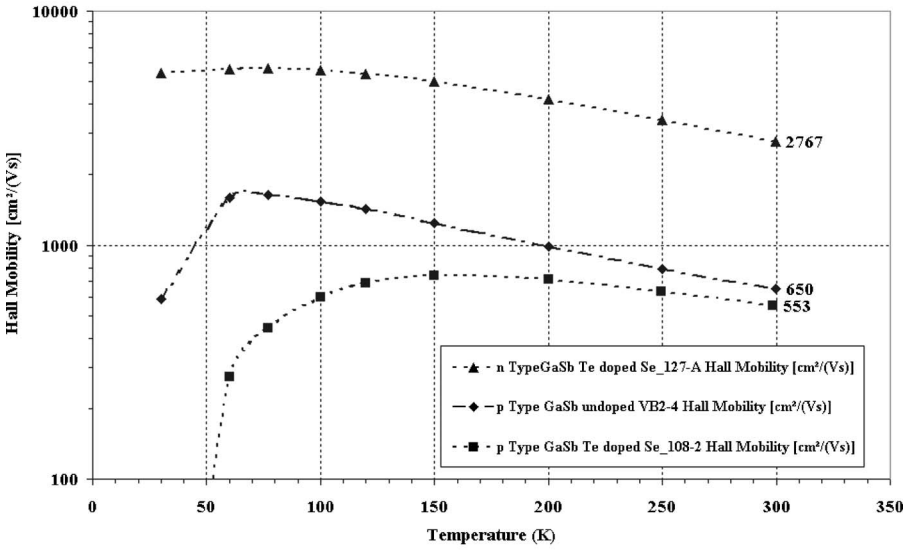

(*b*)

Fig. 2 Carrier concentration (*a*) and Hall mobility (*b*) comparison of *p* and *n* type GaSb samples

probe. For each wafer five measurements were carried out. If we draw the wafer electrical resistivity measurements versus wafer position we obtain a linear variation (Fig. 5).

Wafer 1 is located at the top of the ingot and Wafer 23 is at the bottom. So due to the segregation coefficient of Te into GaSb $k(\mathrm{Cs/Cl})=0.37$ the wafer resistivity decreases during the growth (i.e., the Te concentration increases with the crystal length). Hall measurement on sample Se_127-A cut close to the wafer position 25 gives a value of 4 mΩ cm. The results are in a good agreement with Hall measurement data.

3 Wafer Preparation

3.1 The Gallium Antimonide Treatment Technology at IOFFE. Photovoltaic parameters of semiconductor devices depend to a great extent on the degree of the surface finish and on the preparation quality of semiconductor wafers. For this reason, correct sequence of the wafer treatments and their quality (grinding, polishing, etching, etc.) become important. These preparations may substantially affect subsequent technological processes such as: epitaxy, diffusion, and photolithography.

Semiconductor wafers obtained after cutting from an ingot may present some imperfections such as: roughness, flatness, and spread in thickness. That is why after the cutting process, grinding is a necessary technological operation. Grinding of the gallium antimonide wafers was carried out with the use of a fixed abrasive by means of a diamond disk with grain size of 15–20 μm. The thickness of a ground out layer was not less than 100 μm.

To improve the quality of the semiconductor wafer surface treatment and to decrease the depth of a mechanically damaged layer a polishing process was carried out. A preliminary polishing was done in the same way for both front face and rear side. At this stage a diamond powder with grain size of 1 μm was used for polishing. A polished out layer thickness was 50–70 μm. An additional final polishing combined with etching of the front side was carried out that allowed improvement of the surface quality.

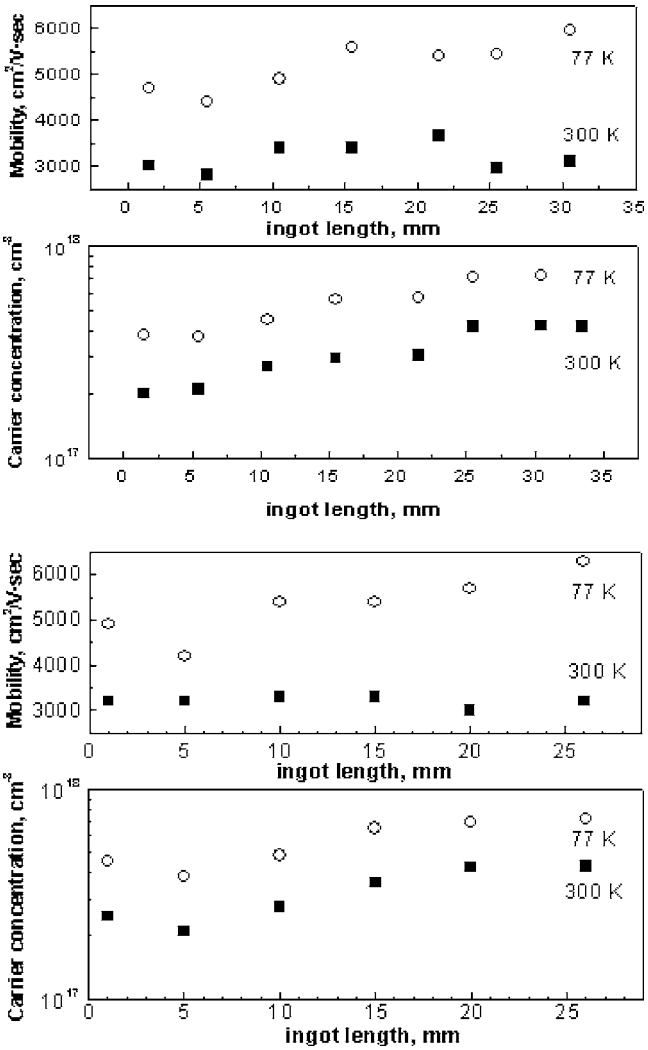

Fig. 3 Hall measurements of free carrier mobility and concentration along *n*-GaSb ingots N91 and N93

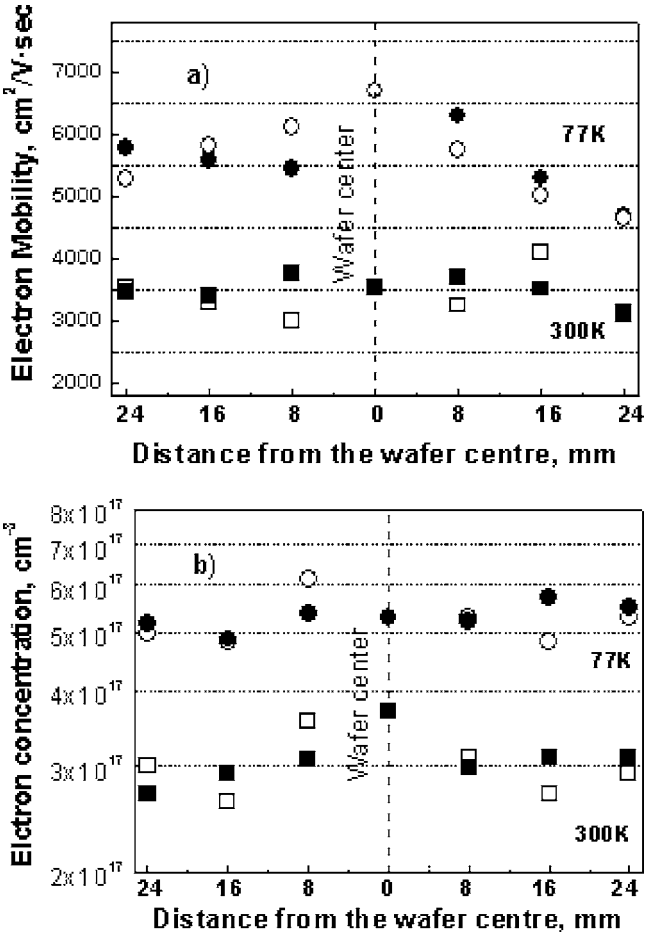

Fig. 4 Free carrier (electron) mobility (*a*) and concentration (*b*) for *n*-GaSb (Te) wafer N36 from the ingot N93 in two perpendicular directions

The polishing time was 1 h resulting in the layer thickness reduction by 5 μm. The final polishing slurry based on zeolite with addition of 40 mL of H_2O_2 and 6 mL of HF was used. The last stage of polishing is of great importance, since it gives the possibility of removing a so called diamond background from the surface of semiconductor wafers arising at the first stage of the surface treatment, and of decreasing the depth of a mechanically damaged layer. The finished wafer thickness after grinding and polishing was 450 μm±5%.

For the epitaxial growth on gallium antimonide wafers, it is necessary to carry out a surface cleaning in order to reduce roughness and to obtain a chemically pure, oxide-free, and atomically flat surface. For this purpose different chemical etchants or an anodic oxidation step with subsequent oxide etching can be used. Due to the fast oxidability of gallium antimonide in the air [21] a more careful approach of surface treatment is required. An additional process besides the chemical etching, namely, a wafer annealing just before the epitaxy, is also a key point.

3.2 The Gallium Antimonide Treatment Technology at CEA. After cutting, wafers were also prepared in a very similar way for grinding and polishing. As mentioned before, a good surface cleaning and etching is of great importance [22]. GaSb wafers were preliminary etched with a $[H_2O:CrO_3:HF]$ solution. Etching time varied from 5 to 10 min. Depending on the concentration, the etching rate was in the range 50–70 mg/mn, which led to a thickness reduction of 5–10 μm per face.

Before and after etching the wafer surface was characterized in terms of surface quality like rugosity. We analyzed a typical 80*80 μm^2 surface.

One can easily see in Figs. 6(*a*) and 6(*b*) the roughness improvement from 36 Å rms down to 3 Å by the etching process. By this way the subdamaged layer induced by the cutting and polishing processes is removed.

After this treatment, GaSb wafers are considered ready for p/n junction realization by the Zn diffusion process.

3.3 Wafer Preparation for LPE and Zinc Diffusion From the Gas Phase. For the wafer treatment two different processes were applied: anodic oxidation with successive etchings out of the oxide film and finally a last step in a special chemical etchant. The choice of one or another treatment procedure for a semiconductor wafer depends on the requirements of subsequent technological processes. For example, to prepare GaSb wafers before the zinc diffusion an anodic oxidation was used. This procedure enabled us to remove precisely thin material layers evenly over the whole wafer surface (both before and after the diffusion process), whereas for the second procedure an irregular wafer etching over the surface was observed. For anodic oxidation, a 3% solution of tartaric acid with ethylenglycol in the relation of 1:2 with addition of NH_4OH was used. For this electrolyte, the etching constant rate of GaSb by anodic oxidation was 1.9 nm/V. The oxide was then removed with hydrochloric acid. Usually the removed layer thickness was not greater than 100 nm. Wafer etching before epitaxial growth was performed with $H_2O:H_2O_2$: 40% tartaric acid

Table 1 GaSb samples and main Hall measurement data

Material	Reference	Orientation	Growth method	Type	Hall mobility results ($cm^2/V\,s$) at 300 K	Density of carriers (atm/cm^3) at 300 K	Resistivity (Ω cm) at 300 K
GaSb undoped	VB2-4	⟨100⟩	VB–LE	*p*	650	1.36×10^{17}	0.069
GaSb:Te	Se_108-2	⟨100⟩	Cz	*p*	553	4.03×10^{16}	0.283
GaSb:Te	Se_108-5	⟨100⟩	Cz	*p*	560	5.00×10^{16}	0.250
GaSb:Te (poly)	Se_125-A	—	Cz	*n*	2780	5.87×10^{17}	0.004
GaSb:Te	Se_127-A	⟨221⟩	Cz	*n*	2767	5.28×10^{17}	0.004
GaSb:Te	N91	⟨100⟩	Mo-Cz	*n*	3200	3.50×10^{17}	0.004
GaSb:Te	N93	⟨100⟩	Mo-Cz	*n*	2800	2.38×10^{17}	0.004

($C_4H_6O_6$): HF (25:25:22:1.5) solution, in combination with HCl (30 s). This treatment allowed removing a thicker surface layer compared to anodic oxidation ($\sim$10 μm). Irregular etching in this case did not have such a negative effect compared to zinc diffusion preparation, since we grew rather thick layers (6–15 μm). Besides, to remove the native oxide from the gallium antimonide surface, which is formed in the air after etching, the wafer annealing at temperatures up to about 600°C for 1/2 h was carried out just before the epitaxy. A complete comparison of the different etching processes is not easy; we hope that future cell performances will give an answer about a more suitable one.

4 Thin Layer Growth and PV Junction Realization

4.1 *p*-type GaSb Growth by LPE Process. Gallium antimonide layers of *p* type grown by the LPE technique were investigated. *p*-type GaSb wafers of 400 μm thickness, (100) oriented, fabricated by CEA were used (samples Se_108). Growth was carried out at 520°C under hydrogen flow in a horizontal quartz reactor. Graphite boats were used as sample holder. Hydrogen was continuously purified by palladium filters. First melt was heated at 850°C for 1 h before epitaxial growth. The layers were not doped during the epitaxy process and were of *p* type. The Hall measurements results of the wafer material gave a mobility μ of 560 $cm^2/V\,s$ at 300 K (410 at 77 K) and a hole concentration *p* of $5\cdot10^{16}$ cm^{-3} at 300 K ($1.5\cdot10^{14}$ cm^{-3} at 77 K).

The x-ray rocking curves were obtained by means of a double-crystal difractometer (with the use of the $K_\alpha Cu$ ($\lambda=1.54$ Å) and an initial monochromator of a perfect Ge crystal ((111) reflection)). This system ensured a 20 in. angular divergency of the incident beam. The full width half maximum (FWHM) of the wafer rocking curve indicates the improvement of the epilayer structural quality compared to the initial wafer.

Since extra peaks are not observed, the wafers and the epitaxial layers have no incorporation of noticeable concentration.

The photoluminescence spectra of wafers and epitaxial layers were measured at 77 K with a 5145 Å Ar laser. The excitation power density was about 500 W/cm^2. Three radiation bands $\sim$0.8 ev, 0.775 ev, and 0.73 eV were observed in the spectrum (Fig. 7).

The 0.8 eV band is associated with the interband recombination, and the 0.775 eV band is usually associated with intrinsic Ga vacancies. The 0.73 eV band is not typical for GaSb, however it is sometimes present in the PL spectrum of *p*-GaSb [23]. The data obtained from the x-ray and photoluminescence investigation allow us to conclude that epitaxial layers thicknesses must be more than 10–15 μm to obtain much better volumetric properties.

Highly doped *p*-GaSb layers are necessary for some TPV devices; for example for tunnel junctions in tandem cells [4], and for decreasing the ohmic contact resistivity. By LPE, experimental dependence of hole concentrations in *p*-GaSb epitaxial layers grown at 350°C from Ga rich melt versus Ge atom content is

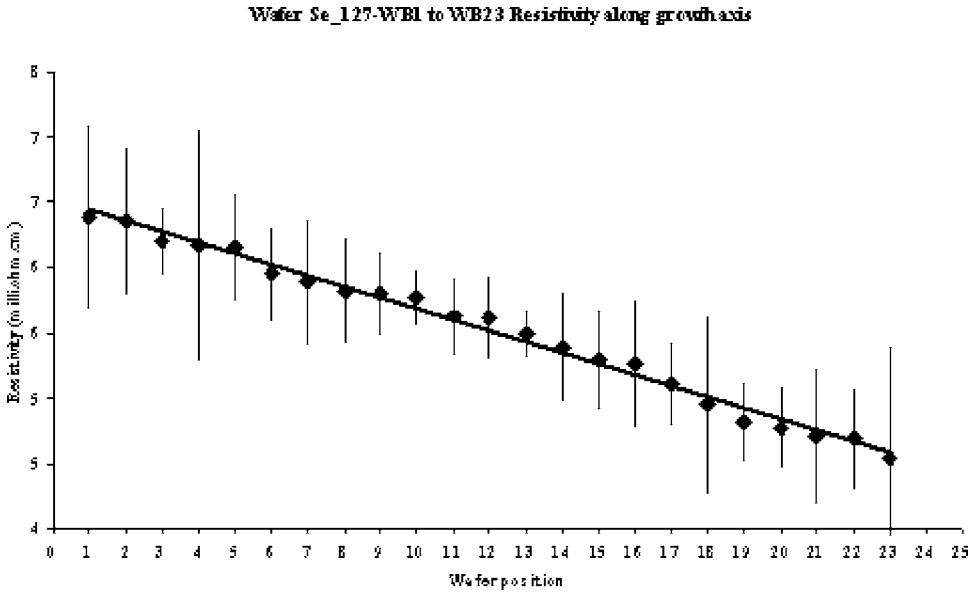

Fig. 5 Resistivity versus position ⟨211⟩ *n* type GaSb:Te sample Se_127 representing 50 mm of the ingot

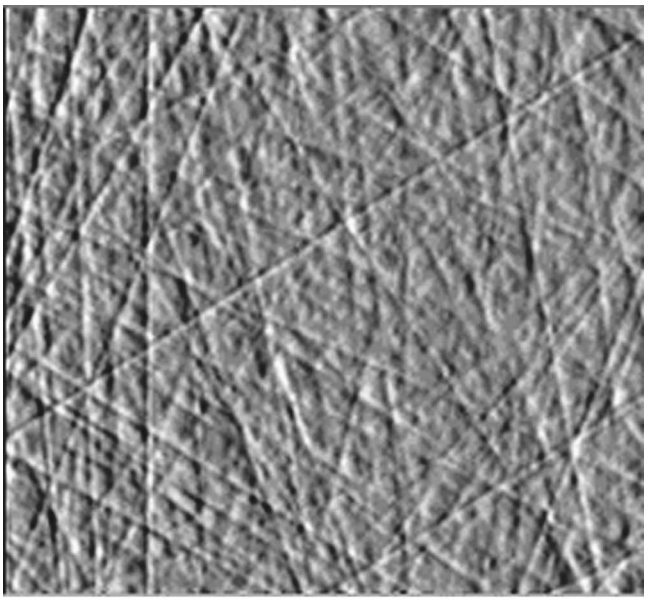

Fig. 6 Surface quality ⟨100⟩ *p* type GaSb:Te sample Se_108

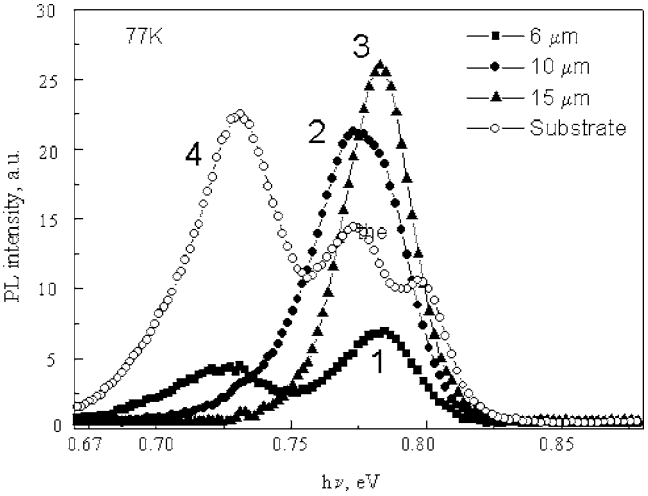

Fig. 7 Photoluminescence spectra of a *p*-GaSb wafer (4) and of epitaxial (LPE) *p*-GaSb layers of different thicknesses: 1–6 μm, 2–10 μm and 3–15 μm

obtained. From this dependence, the solubility isotherm has linear behavior for all ranges of measured hole concentration in GaSb (Ge) layers.

4.2 *n*-type GaSb Growth by LPE Process. The main parameters of *n*-GaSb substrates for LPE growth are: doping by Te, $(2-8)\cdot 10^{17}$ cm^{-3}; electron mobility of $(3-5)\cdot 10^3$ cm^2/V s (300 K); dislocations density $N_{Dis} < 5\cdot 10^3$ cm^{-2}; orientation (100); and thickness of 450 μm±20 μm.

LPE growth conditions of *n*-GaSb were the same as for *p*-GaSb epilayers. Figure 8 presents the dependence of charge carriers' mobility versus the doping level for *n*-GaSb epitaxial layers doped by Te.

If we compare ingot and epitaxial layer mobility one may note that in the epitaxial layers the mobility values are higher: 4000–4500 cm^2/V s at $n=2-4\cdot 10^{17}$ cm^{-3} than in the wafer (Fig. 8), in which the mobility was 3000–3500 cm^2/V s. Thus, the LPE technique allows us to grow layers with higher carrier mobility. This may be explained by the smaller amount of defects compared to those in the ingot material. The layers with high mobility and doping level in the range of $(2-6)\cdot 10^{17}$ cm^{-3} (300 K) were used for creation of the photosensitive region of GaSb photoconverters. Defects that appeared in the material led to an increase of the leakage currents in the region of the *p-n* junction, which affect the separation of generated charge carriers. Heavily doped GaSb n^+ layers ($\geq 10^{18}$ cm^{-3}) were grown (Fig. 8) for contact layers, which allowed us to decrease the ohmic contact resistivity to about 10^{-6} Ω cm^2.

4.3 GaSb Grown by MOCVD Process. Epitaxial growths were performed inside AIX200 installation with a horizontal reactor configuration. Pressure in the reactor was kept at 100 mbar during growth. Heating of the wafer holder was done by infrared lamps. The growth temperature was in the range of 550–600°C. Hydrogen purified in a palladium filter, with the dew point not more than −100°C was used as a gas carrier. Triethylgallium (TEGa) has been chosen as a source of the third group element, since its pyrolytic cracking is not accompanied by formation of the radical able to react. Trimethylantimony (TMSb) has been chosen as a source of the fifth group element. The choice of this metalorganic compound is justified by more effective degrading at 550°C compared to that of stibnine (SbH3) and by the results of

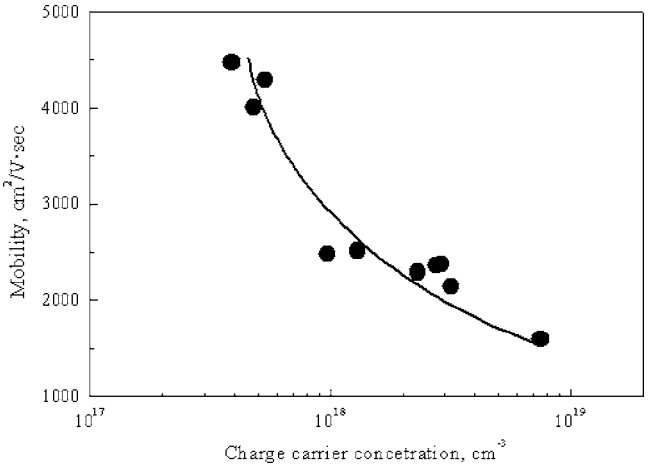

Fig. 8 Dependence of the charge carrier mobility on electron concentration in the epitaxial *n*-GaSb:Te layers at 300 K

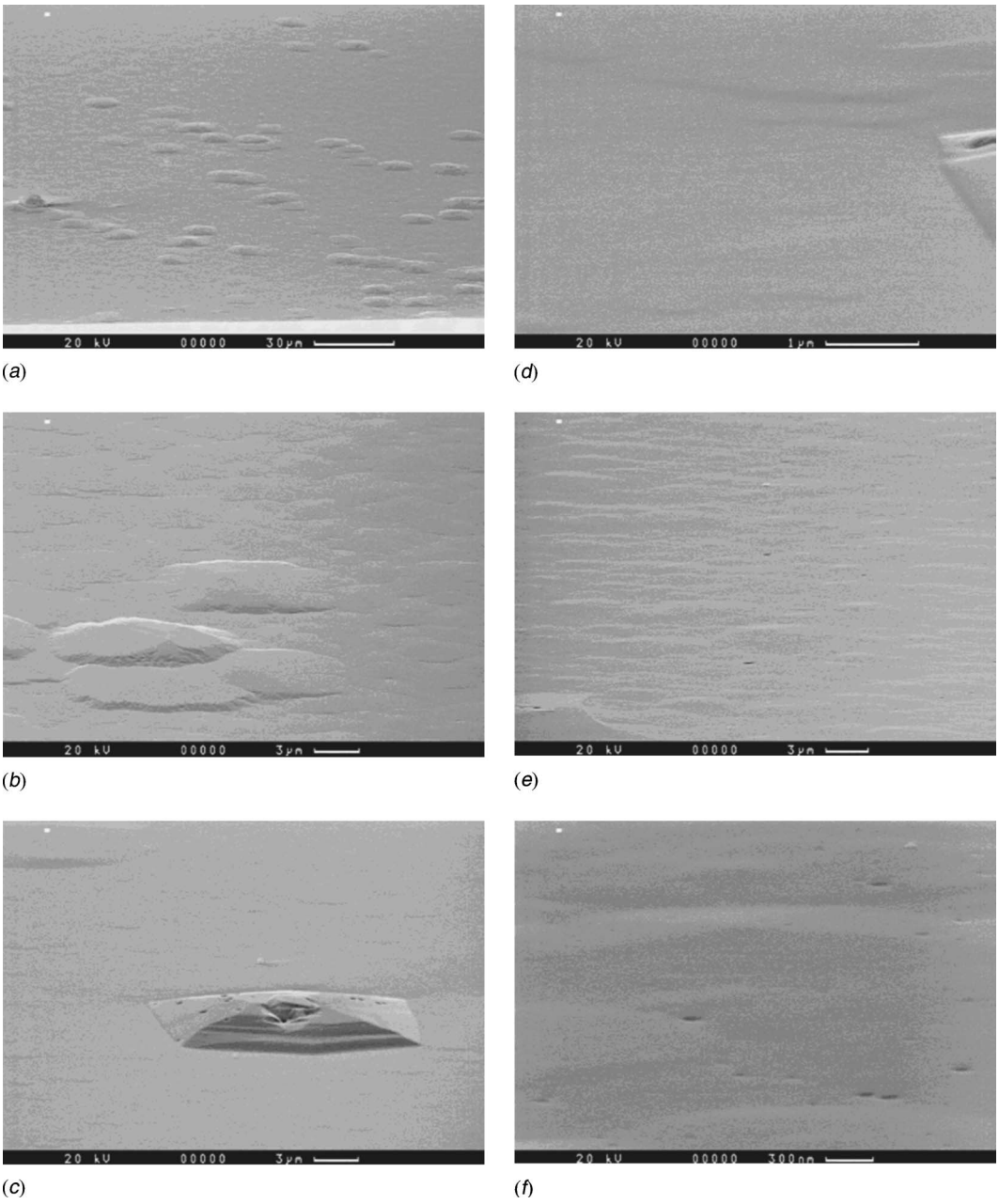

Fig. 9 The surface morphology of GaSb epitaxial layers (the morphology was estimated by means of electronic microscopes): (*a*),(*b*) sample 1; (*c*),(*d*) sample 2; (*e*),(*f*) sample 5

the work in Refs. [24,25].

In our work, the layers were grown on a *n*-GaSb:Te wafer oriented in the (100) plane, with concentration $n = 3-5 \cdot 10^{17}$ cm^{-3}. Before epitaxy GaSb wafers were degreased by CCl_4 vapor and isopropyl alcohol for 2 h. The degreased GaSb wafers were etched in sulfur–peroxide $H_2SO_4-H_2O_2-H_2O$ (5:1:1) for 30 s at room temperature. The epitaxial growth duration was 60–90 min.

The influence of GaSb surface preparation on MOCVD layers properties has been studied.

4.3.1 Treatment of GaSb *Substrates in Concentrated* HCl. Degreased GaSb wafers were treated in concentrated HCl for 5 min. The layer was grown with a V/III species ratio equal to 1.8 under a hydrogen flow of 6.5 slpm. The epitaxial layer thickness was about 1.7 μm after 1 h growth.

Hillocks were observed on the surface (Figs. 9(*a*) and 9(*b*)). Their concentration varied over the surface: few hillocks are present at wafer edges. On average the concentration of such defects was about $6 \cdot 10^3$ cm^{-2}. Defects formation is, apparently, associated with an unsatisfactory treatment of the wafer surface since the concentrated hydrochloric acid removes only the oxide film.

4.3.2 Treatment of GaSb *Substrates by Anodic Oxidation*. The wafers were first treated by anodic oxidation in an electrolyte (H_2O:40% tartaric acid: NH_4OH: ethylene glycol) at voltage up to 50 V and current of 2–3 mA, and then in concentrated HCl for 2–3 min. Before epitaxial growth, the wafer was held at 550°C under H_2 flow for 10 min removing the oxide formed on the GaSb surface [26]. The layers were grown with a V/III ratio of 2.5. The change of this ratio is associated with the selection of technological regimes that enabled us to obtain more qualitative layers. The growth rate was 1.65 μm/h.

Table 2 Types of chemical treatments of a GaSb wafer material

GaSb treatment	Treatment in HCl	Anodic oxidation	Etching
Etching depth, (μm)	Only oxide removal	0,1–0,2	6–8
Defect concentration, (cm^{-2})	$6\cdot10^3$	$5\cdot10^2$	$2\cdot10^2$

Small pyramids were observed on the epitaxial layer surface (Figs. 9(*c*) and 9(*d*)). Their density also varied over the surface, similar to the previous case, where the defects density was smaller by $\sim 5\cdot10^2$ cm^{-2}. A combination of anodic oxidation and annealing allowed for preparation of good wafer surface for epitaxy and better epilayer quality. Due to this process the mechanically damaged layer was partially removed. This probably reduced the defect density at the growth interface.

4.3.3 Treatment of GaSb *Substrates in an Etchant*. For a more effective etching the degreased GaSb wafers were first treated in concentrated HCl for 5 min, and second in the etchant $H_2O-H_2O_2$ 40% tartaric acid–HF(25:25:22:1.5) for 1 min, and finally once more in concentrated HCl for 1 min. The epilayer was grown with a V/III of 2.5. Before the growth the wafers were annealed at 550°C.

The surface presented a small relief, which apparently, seems, associated with the fact that the oxide film formed on the wafer surface during the load in the reactor (Figs. 9(*e*) and 9(*f*)).

Therefore GaSb wafer treatment only with concentrated hydrochloric acid is not effective for MOCVD growth. Etching in $H_2O-H_2O_2$ 40% tartaric acid–HF(25:25:22:1.5) in combination with treatment in concentrated HCl and annealing in hydrogen is more effective, at a condition where the mechanically damaged layer and the oxide film were previously fully removed. This is indicated by the reduction defects concentration on the surface from $6\cdot10^3$ down to $2\cdot10^2$ defects/cm^2. The results of a different kind of GaSb wafer treatment before the epitaxy are presented in Table 2.

In Fig. 10 and Table 3, the dependence of the photoluminescence intensity on the ratio of the components in the gas phase is presented. The photoluminescence peak intensity rises, when the ratio changes from 1 to 2, and drops by increasing the ratio from 1.8 to 3. By increasing the V/III ratio over 3 the PL intensity decreases. Following these observations, the best working range of the V/III ratio, for growing high-quality epitaxial layers, is 1.5–2.2.

The crystalline perfection of the obtained layers was also estimated by means of the x-ray measurements. FWHM for the gallium antimonide epitaxial layers decreases by two times compared with the wafer.

4.4 *p/n* Junction Obtained by Zinc Diffusion in Vapor Phase. *p/n* junction elaboration on a *n* type GaSb:Te wafer by the vapor phase Zn diffusion process is one of the most common and "simplest" approaches for TPV applications [1–5,26–28]. Several wafers 2 in. in diameter were installed in a cylindrical silica ampoule with a small amount of high-purity zinc piece.

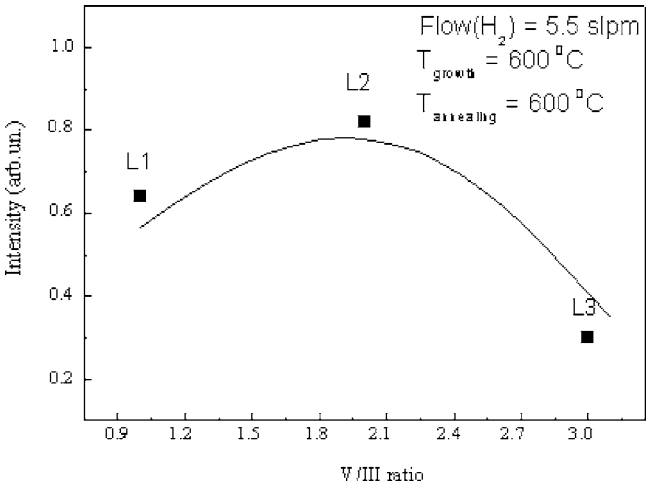

Fig. 10 The photoluminescence intensity versus the ratio of elements

After pumping under secondary vacuum, the ampoule was sealed. As the best Zn diffusion depth is in the range from 0.5 μm to 2.5 μm we adapted our furnace parameters for operation at 480–520°C with diffusion duration between 1 h and 3 h of diffusion. Samples were processed with a good temperature control because, as a sharp Zn profile is required, we must also ensure that no zinc condensations will occurred during the cooling phase. Then a *p/n* junction was obtained. For establishing this process some secondary ion mass spectrometry (SIMS) analyses were done.

We can see in Fig. 11(*a*) the Zn diffusion profile obtained on sample Se_108-3 at 500°C after 3 h. Since both front and rear wafer faces are Zn diffused, a polishing process of the rear face must be performed for removing this unnecessary *p/n* junction before back contact realization. The Te measured profile (Fig. 11(*b*)), appears to be constant inside the bulk GaSb and the value is close to ICP results and Hall measurements.

After diffusion samples are ready for TPV cells manufacturing. This step is under realization.

5 Conclusion

In this paper, we investigated GaSb:Te material properties for thermophotovoltaic applications. We first compared bulk material grown by different methods from different teams. The gallium antimony Czochralski growth method was developed and GaSb single crystals up to 4.2 kg were obtained. As the tellurium concentration level specification is of great importance, we carried out Hall measurements on *p*-type and *n*-type GaSb:Te samples. Mobility up to 3200 cm^2/V s (300 K) for a carrier concentration of 3.510^{17} atm/cm^3 for *n*-type GaSb:Te oriented ⟨100⟩ was measured. Mobility differences between undoped, *p*-type and *n*-type GaSb:Te were reported as a function of temperature. Radial carrier concentration and mobility variation within a 2 in. sample was 20–30%. Carrier concentration and resistivity variations with

Table 3 PL Intensity of a GaSb layers in dependence from type of chemical treatment of wafers and *V/III* ratio during MOCVD process

Sample No.	V/III	Type of treatment	Intensity PL (arb.units)	T_{growth} (°C)	$T_{annealing}$ (°C)	Flow (H_2) (slpm)
1	1.8	Treatment in HCl	0.23	550	550	6.5
2	2.5	Anode oxidation	0.18			
4	3	Etching	0.19			
5	1.8	Etching	1.01			

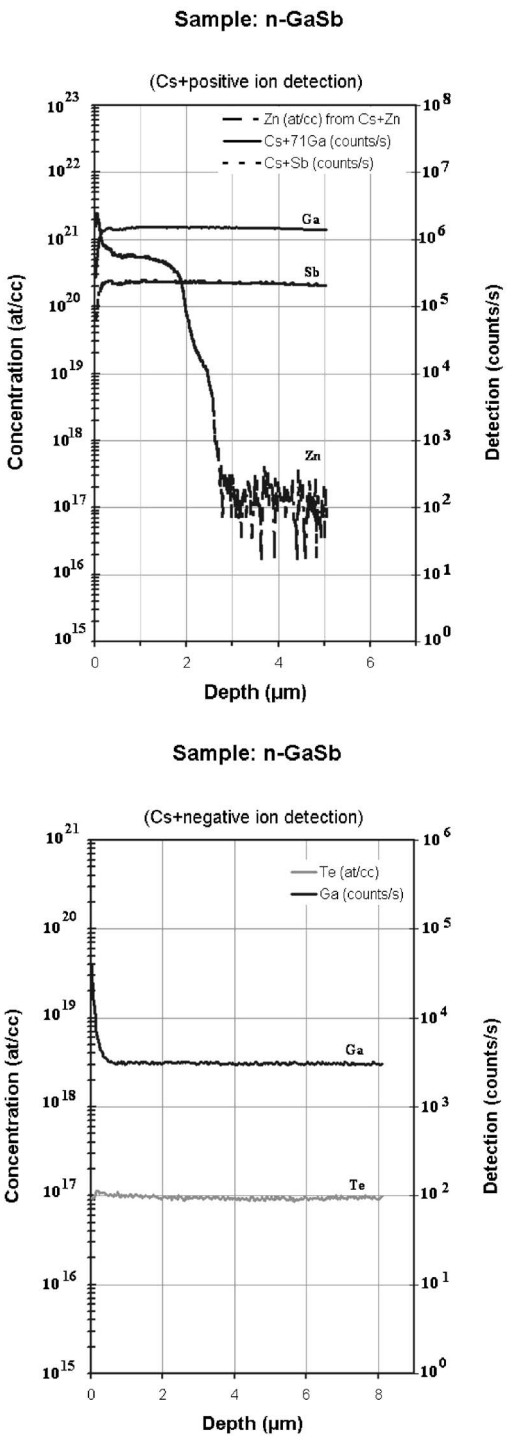

Fig. 11 SIMS measurements on *n*-GaSb:Te sample Se_127 after Zn diffusion

wafer position were also presented. These material properties were mainly influenced by the Te incorporation inside GaSb during growth.

After growth, GaSb wafer preparation is an important step for p/n or n/p junction realization. Different cutting, grinding, and polishing processes were successfully applied with some GaSb specificity for the final chemico-mechanical process. Wafers were then chemically etched for removing subdamaged layers and also surface pollution. The etchant choice depends on the subsequent method for p/n junction. Mean wafer rugosity of 3 Å ($80*80\ \mu m^2$) is obtained on *n*-type GaSb before the zinc diffusion process.

For the LPE process an anodic oxidation method was used in order to control accurately the part of the sample removed before growth. For the LPE process *n*-type GaSb epitaxial layers on a *p*-type wafer up to 15 μm were obtained. Layer qualities were characterized by x-ray rocking curves and photoluminescence spectra. Epilayer quality improvement was observed for *p* type GaSb of 15 μm. For *p* type GaSb doped in the range $10^{18}-10^{20}$ holes/cm^3, a linear variation of the Ge melt concentration was found. For *n* type epilayers by LPE, mobility increased from 3000–3500 cm^2/V s to 4000–4500 cm^2/V s. For the heavily doped *n*+ layer, concentration up to 8.10^{18} atm/cm^3 allowed us to decrease the resistiviy contact to $10^{-6}\ \Omega\ cm^{-2}$.

For epitaxial growth by MOCVD, specific wafer preparation was necessary. Among the different etching mixtures tested the best results were obtained with $H_2O-H_2O_2$ 40% tartaric acid–HF(25:25:22:1.5) in combination with treatment in concentrated HCl and annealing under hydrogen atmosphere. The best crystalline layers analyzed with x-ray rocking curve were obtained with a III/V ratio in the range 1.5–2.2.

For a p/n junction obtained by zinc diffusion in vapor phase on *n*-type GaSb:Te, the best proposed parameters for diffusion were temperatures of 480–520 °C and duration from 1 to 3 h. The zinc profile obtained by SIMS showed a sharp p/n junction at 2 μm.

TPV devices are now under fabrication. Nevertheless a continuous material improvement conjugated with a good wafer surface preparation and an accurate set of characterization methods appeared to be crucial for a better understanding of the cell performance.

Acknowledgment

This work has been partially supported by the European Commission through funding of the project FULLSPECTRUM (Ref. No. SES6-CT-2003-502620). The authors would like to thanks all TPVCELL partners (Ref. No. RTN2-2001-0454) for very fruitful discussions.

References

[1] Frass, L. M., Girard, G. R., Avery, B. A., Arau, V. S., Sundaram, V. S., Tompson, S. M., and Gee, J. M., 1989, "GaSb Booster Cells for Over 30% Efficient Solar-Cell Stacks," J. Appl. Phys., **66**(8), pp. 3866–3870.

[2] Khvostikov, V. P., Sorokina, S. V., and Shvarts, M. Z., 1995, "GaSb Based Solar Cells for Concentrator Tandem Application," *Proc. 13th European Photovoltaic Solar Energy Conference and Exhibition*, Nice, France, pp. 61–64.

[3] Bett, A. W., Dimroth, F., Stollwerck, G., and Sulima, O. V., 1999, "III-V Compounds for Solar Cell Applications," Appl. Phys. A, **69**, pp. 119–129.

[4] Shvarts, M. Z., Andreev, V. M., Khvostikov, V. P., Larionov, V. R., Rumyantsev, V. D., Sorokina, S. V., Vasil'ev, V. I., Vlasov, A. S., and Chosta, O. I., 1998, "GaSb/InGaAsSb Tandem Thermophotovoltaic Cells for Space Applications," *Proc. 5th European Space Power Conference*, Tarragona, Spain, pp. 527–532.

[5] Martin, D., and Algora, C., 2004, "Theoretical Comparison Between Diffused and Epitaxial GaSb TPV Cells," *Proc. 6th Conference on Thermophotovoltaic Generation of Electricity*, Freiburg, Germany, A. Gopinath et al., eds., American Institute of Physics, Melville, NY, pp. 311–319.

[6] Kumagawa, M., 1978, "Observations of Microfacets Near Irregularly Remelted Surfaces in Pulled GaSb Crystals," J. Cryst. Growth, **44**(3), pp. 291–296.

[7] Miyazawa, S., Kondo, S., and Naganuma, M., 1980, "A Novel Encapsulant Material for LEC Growth of GaSb," J. Cryst. Growth, **49**(4), pp. 670–674.

[8] Hársy, M., Görög, T., Lendvay, E., and Koltai, F., 1981, "Direct Synthesis and Crystallization of GaSb," J. Cryst. Growth, **53**(2), pp. 234–238.

[9] Kondo, S., and Miyazawa, S., 1982, "Low Dislocation Density GaSb Single Crystals Grown by LEC Technique," J. Cryst. Growth, **56**(1), pp. 39–44.

[10] Ohmori, Y., Sugii Shin-ichi Akai, K., and Matsumoto, K., 1982, "LEC Growth of Te-Doped GaSb Single Crystals With Uniform Carrier Concentration Distribution," J. Cryst. Growth, **60**(1), pp. 79–85.

[11] Sunder, W. A., Barns, R. L., Kometani, T. Y., Parsey, J. M., and Laudise, R. A. Jr., 1986, "Czochralski Growth and Characterization of GaSb," J. Cryst. Growth, **78**(1), pp. 9–18.

[12] Doerschel, J., and Geissler, U., 1992, "Characterization of Extended Defects in Highly Te-Doped ⟨111⟩ GaSb Single Crystals Grown by the Czochralski Tech-

nique," J. Cryst. Growth, **121**(4), pp. 781–789.
[13] Watanabe, A., Tanaka, A., and Sukegawa, T., 1993, "GaSb Solution Growth by the Solute Feeding Czochralski Method," J. Cryst. Growth, **128**(1–4), pp. 462–465.
[14] Boiton, P., Giacometti, N., Duffar, T., Santailler, J. L., Dusserre, P., and Nabot, J. P., 1999, "Bridgman Crystal Growth and Defect Formation in GaSb," J. Cryst. Growth, **206**(3), pp. 159–165.
[15] Duffar, T., Dusserre, P., and Giacometti, N., 2001, "Growth of GaSb Single Crystals by an Improved Dewetting Process," J. Cryst. Growth, **223**(1–2), pp. 69–72.
[16] Van Der Meulen, Y. J., 1967, J. Phys. Chem. Solids, **28**, p. 25.
[17] Dutta, P. S., and Ostrogorsky, A. G., 1998, "Nearly Diffusion Controlled Segregation of Tellurium in GaSb," J. Cryst. Growth, **191**(4), pp. 904–908.
[18] Voloshin, A. E., Nishinaga, T., Ge, P., and Huo, C., 2002, "Te Distribution in Space Grown GaSb," J. Cryst. Growth, **234**(1), pp. 12–24.
[19] Kunitsyn, A. E., Chaldyshev, V. V., Mil'vidskaya, A. G., and Mil'vidskii, M. G., 1997, "Properties of Tellurium-Doped Gallium Antimonide Single Crystals Grown From Nonstoichiometric Melt," Semiconductors, **31**(8), pp. 806–808.
[20] Pino, R., Ko, Y., and Dutta, P. S., 2004, "Enhancement of Infrared Transmission in GaSb Bulk Crystals by Carrier Compensation," J. Appl. Phys., **96**(2), pp. 1064–1067.
[21] Papis, E., Kudla, A., Piotrowski, T. T., Golaszewska, K., Kaminska, E., and Piotrowska, A., 2001, "Ellipsometric Investigations of (100) GaSb Surface under Chemical Etching and Sulfide Treatment," Mater. Sci. Semicond. Process., **4**, pp. 293–295.
[22] Schegl, T., Sulima, O. V., and Bett, A. W., 2004, "The Influence of Surface Preparation on Zn Diffusion Processes in GaSb," *Proc. 6th Conference on Thermophotovoltaic Generation of Electricity*, Freiburg, Germany, A. Gopinath et al., eds., American Institute of Physics, Melville, NY, pp. 396–403.
[23] Kyuregyan, A. S., Lazareva, I. K., Stuchebnikov, V. M., and Yunovich, A. E., 1972, "Photoluminescence of the GaSb for Large Level Stimulation," Sov. Phys. Semicond., **6**(2), pp. 242–247.
[24] Wang, C. A., Salim, S., Jensen, K. F., and Jones, A. C., 1997, "Characteristics of GaSb Growth Using Various Gallium and Antimony Precursors," J. Cryst. Growth, **170**, pp. 55–60.
[25] Wang, C. A., Shiau, D. A., and Lin, A., 2004, "Preparation of GaSb Substrates for GaSb and GaInAsSb Growth by Organometallic Vapor Phase Epitaxy," J. Cryst. Growth, **261**, pp. 385–392.
[26] Bett, A. W., Kesser, S., and Sulima, O. V., 1997, "Study of Zn Diffusion into GaSb from the Vapour and Liquid Phase," J. Cryst. Growth, **181**, pp. 9–16.
[27] Sulima, O. V., and Bett, A. W., 2001, "Fabrication and Simulation of GaSb Thermophotovoltaic Cells," Sol. Energy Mater. Sol. Cells, **66**, pp. 533–540.
[28] Simcock, M. N., Santailler, J.-L., Dusserre, P., and Giacometti, N., 2004, "Zinc Diffusion in GaSb for Thermophotovoltaic Cell Applications," *Proc. 6th Conference on Thermophotovoltaic Generation of Electricity*, Freiburg, Germany, A. Gopinath et al., eds., American Institute of Physics, Melville, NY, pp. 303–309.